

Received: 2020.12.24

Accepted: 2021.02.08

Available online: 2021.02.21

Published: 2021.05.02

Parameters Indicating Development of Influenza-Associated Acute Necrotizing Encephalopathy: Experiences from a Single Center

Authors' Contribution:
Study Design A
Data Collection B
Statistical Analysis C
Data Interpretation D
Manuscript Preparation E
Literature Search F
Funds Collection G

AE 1 **Suyun Li***
AE 2 **Dandan Hu***
AE 1 **Peiqing Li***
AE 3 **Weiqiang Xiao***
ACE 4 **Huixian Li***
C 1 **Guangming Liu**
C 1 **Yongling Song**
C 2 **Shuyao Ning**
F 1 **Qiuyan Peng**
F 5 **Danyang Zhao**
F 5 **Minxiong Situ**
B 1 **Wanqi Li**
B 1 **Peiqun Wu**
B 1 **Jipeng Zheng**
B 1 **Yueting Liu**
B 1 **Lin Hu**

1 Department of Pediatric Emergency Medicine, Guangzhou Women's and Children's Medical Center, Guangzhou Medical University, Guangzhou, Guangdong, P.R. China
2 Department of Pediatric Neurology, Guangzhou Women's and Children's Medical Center, Guangzhou Medical University, Guangzhou, Guangdong, P.R. China
3 Department of Radiology, Guangzhou Women's and Children's Medical Center, Guangzhou Medical University, Guangzhou, Guangdong, P.R. China
4 Data Statistics Center, Guangzhou Women's and Children's Medical Center, Guangzhou Medical University, Guangzhou, Guangdong, P.R. China
5 Department of Disease Control and Prevention, Guangzhou Women's and Children's Medical Center, Guangzhou Medical University, Guangzhou, Guangdong, P.R. China

B 1 **Pengfei Wang**
B 1 **Zhengbin Hu**
D 1 **Wencheng Ma**
D 1 **Jun Shen**
A 2 **Sida Yang**

* Suyun Li, Dandan Hu, Peiqing Li, Weiqiang Xiao and Huixian Li contributed equally to this work

Corresponding Author:

Sida Yang, e-mail: yangsida2013@126.com

Source of support:

This work was supported by: National Natural Science Foundation of China (No. 81801206); Science and Technology Key Project for People's Livelihood of Guangzhou, China (No. 201803010026); Medical Science and Technology Research Foundation of Guangdong, China (No. A2019373); Guangdong Natural Science Foundation [No.2020A1515010014]; and Innovative Project of Children's Research Institute, Guangzhou Women's and Children's Medical Center, China (No. Pre-NSFC-2018-004, Pre-NSFC-2018-008, and IP-2018-006)

Background: Influenza-associated acute necrotizing encephalopathy (IANE) can be lethal and disabling and have a sudden onset and deteriorate rapidly but lacks early diagnostic indicators. We aimed to examine the early clinical diagnostic indicators in children with IANE.

Material/Methods: Acute influenza patients were grouped according to their clinical manifestations: flu alone (FA), flu with febrile seizure (FS), influenza-associated encephalopathy (IAE), and IANE. The clinical features, biomarkers, neuroelectrophysiological results, and neuroimaging examination results were compared.

Results: A total of 31 patients were included (FA (n=4), FS (n=8), IAE (n=14), and IANE (n=5)). The IANE group, whose mean age was 3.7 years, was more likely to show rapid-onset seizure, acute disturbance of consciousness (ADOC), Babinski's sign, and death/sequela. More patients in the IANE group required tracheal intubation mechanical ventilation and received intravenous immunoglobulins (IVIG) and glucocorticoids. The alanine aminotransferase (ALT), aspartate transaminase (AST), and lactate dehydrogenase (LDH) levels in the IANE group were significantly higher than in the FS and IAE groups. The aquaporin-4 (AQP-4) antibody and malondialdehyde (MDA) levels in the serum and cerebrospinal fluid (CSF) were notably higher in IANE patients in the acute stage compared with FS and IAE patients. All patients in the IANE group had positive neuroimaging findings.

Conclusions: Early clinical warning factors for IANE include rapid-onset seizures in patients under 4 years of age, ADOC, and pathological signs. Increased AQP-4 antibodies and MDA levels in CSF might contribute to early diagnosis. Early magnetic resonance venography (MRV) and susceptibility-weighted imaging (SWI) sequences, or thrombelayography to identify deep vein thrombosis, might indicate clinical deterioration.

Keywords: **Brain Injuries • Child • Early Diagnosis • Influenza, Human**

Full-text PDF: <https://www.medscimonit.com/abstract/index/idArt/930688>



2890

2

7

60

Background

Influenza-associated acute necrotizing encephalopathy (IANE) is an extremely dangerous and lethal condition with acute onset and rapid progression [1-9]. Its diagnosis is mainly based on brain imaging [10-12]. Patients with IANE can miss the opportunity of neuroimaging in the acute phase because of the patients' conditions. Because of the imaging lag of brain lesions, neuroimaging might not provide the clinical judgment of early brain lesion consistent with the actual condition. Researchers have constantly been trying to find biological indicators that are relevant to the diagnosis of IANE. Still, the pathogenesis of IANE has not been clear, and there has been no breakthrough in finding IANE-related biomarkers. After reviewing both the relevant reports and the brain pathology of IANE non-survivors, we analyzed the clinical manifestation, biomarkers, neuroimaging, and neuroelectrophysiology examination results of patients with IANE to explore the early clinical diagnostic indicators of IANE, as well as the high-risk factors.

Material and Methods

Study Site

The study was carried out in Guangzhou Women's and Children's Medical Center, Guangzhou, Guangdong Province, southern China, using 233 specimens collected into the "Guangzhou Women's and Children's Medical Center Biobank" from May 2018 to January 2019.

Among these patients, 33 were diagnosed with acute influenza and did not meet the exclusion criteria. They were divided into 4 groups: 1) the FA group (n=4) contained children with influenza without neurological symptoms; 2) the FS group (n=8) contained children with influenza and febrile seizure; 3) the IAE group (n=14) contained children with influenza-associated encephalopathy; 4) the IANE group (n=5) contained children with influenza-associated acute necrotizing encephalopathy. The exclusion criteria were: 1) multiple infections, such as combined RSV, CMV, EBV, MP, varicella, measles, and bacterial infection; 2) severe central nervous system deformities, such as mass, tumor, trauma, cerebral vascular malformation, meningitis, and pachygyria; 3) basic diseases that can cause brain lesions, such as mitochondrial brain disease, SLE encephalopathy, hypoxic-ischemic encephalopathy, purulent meningitis, brain abscess, cerebral hemorrhage; and 4) basic diseases such as cerebral palsy and hydrocephalus. All information was extracted from the structured electronic medical record system (EMRS).

Laboratory Tests

Laboratory Tests of Influenza Virus

For influenza virus testing, real-time reverse transcription-polymerase chain reaction (rRT-PCR) was performed using the influenza virus A/B dual fluorescence quantitative RT-PCR kit (Guangdong Guanyin Pharmaceutical Technology Co. LTD, China). The influenza virus A subtype identification was performed using the real-time RT-PCR kit (Dan Gene Co., Ltd, Sun Yat-Sen University, China).

Automatic Biochemistry System

For clinical routine biochemical testing, an automatic analyzer (Automatic Analyzer 7600, Hitachi High-Technologies Corporation) was used.

Specific Biochemical Tests

The specimens of plasma and cerebrospinal fluid (CSF) were tested in the included cases. The equipment included: a microplate reader (Thermo Fisher Scientific, Multiscan MK3) and a fluorescence analyzer (Perkin Elmer, Victor X5). The reagents used were Cyt-C ELISA Kit (Cusabio, Wuhan, China, No: CSB-E08530h), Apo-ONE® Homogeneous Caspase-3/7 Assay (Promega, USA, No: G7790), Amplex® Red Hydrogen Peroxide/Peroxidase Assay Kit (Invitrogen, USA, No: A22188), AA (PDGF-AA) ELISA Kit (Cusabio, Wuhan, China, No: CSB-E17143h), VEGF ELISA Kit (MultiSciences, Hangzhou, China, No: 70-EK1832), Human aquaporin-4 antibody (AQP-4 Ab) ELISA Kit (Cusabio, Wuhan, China, No: CSB-E13568h), Human anti-NMDAR Antibody ELISA Kit (Fine Test, Zurich, Switzerland, No: EH4166), Human MOG (Myelin-oligodendrocyte glycoprotein) ELISA Kit (Fine Test, Zurich, Switzerland, No: EH0896), and Lipid Peroxidation MDA Assay Kit (Beyotime Biotechnology Co., Ltd., Shanghai, China, No: S0131).

Neuroimaging and Neuroelectrophysiology Examination

Magnetic Resonance Imaging (MRI)

MRI was performed by super-conducting 1.5-T (Achieva; Philips, Netherlands) and 3.0-T (Skyra; Siemens Medical Solution, Germany) MR units and standard head coils. Routine 1.5-T MR imaging included the following sequences: sagittal and transverse T1-weighted spin-echo (repetition time ms/echo time ms, 450/11; number of signals acquired, 2), transverse T2-weighted fast spin-echo (3200-4500/90-120; number of signals acquired, 3-4), and transverse fluid-attenuated inversion recovery (repetition time msec/echo time msec/inversion time msec, 8000/120/2300). Routine 3.0-T MRI included the following sequences: sagittal and transverse T1-TRIM

dark-fluid (repetition time msec/echo time msec, 2000/9; number of signals acquired, 6), transverse T2-weighted fast spin-echo (4200/110; number of signals acquired, 19), and transverse fluid-attenuated inversion recovery (repetition time msec/echo time msec/inversion time msec, 8000/111/2360). Other pulse sequences were performed as clinically indicated.

Computed Tomography (CT)

CT imaging was performed with a 64-slice CT (Brilliance; Philips, Netherlands & Aquilion; Toshiba, Japan). Scan parameter: 120 kV, 100 mA, slice thickness 5 mm, slice gap 5 mm.

Electroencephalography (EEG)

Continuous EEG was recorded using a 32-channel NicoletOne EEG. Each subject was set with the 19 montages in the scalp (corresponding to the positions in the standard 10-20 montage) and was recorded for 12 h.

Statistical Analysis

SAS 9.4 for Windows (SAS Institute, Inc., Cary, USA) was used for data analysis. Categorical variables are presented as numbers (percentage) and were compared using Fisher's exact test. Continuous data are presented as means (standard deviation, SD) or medians (interquartile range, IQR) and were analyzed using one-way ANOVA with multiple comparisons with a Bonferroni adjustment or the Kruskal-Wallis test followed by the Dunn post-test depending on the distribution ($\alpha=0.05$).

Ethics Approval and Consent to Participate

The biobank and the present study were approved by the ethics committee of Guangzhou Women and Children Medical Center. Banking of the specimens was done after obtaining the written informed consent of the patients' legal guardians.

Limitations

The study had some limitations. First, the cases were only from the Guangzhou Women's and Children's Medical Center, and the generalizability might be challengeable. In addition, the sample size was small, precluding any reliable calculation of sensitivity and specificity. Secondly, we only analyzed clinical facts and biomarkers associated with the disease, which might not cover all possibilities. Further research will be needed to improve the prospective cohort design and increase the sample size.

Results

Demographic, Clinical Features, and Treatment

All patients with IANE had radiological signs of acute necrotizing encephalopathy on brain imaging and were positive for the influenza virus. In the present study, one patient in the IANE group died at 20 days after onset. Three patients had sequela, including disturbance of consciousness, language barrier, movement disorder, no communication, no recognition, involuntary movement, and cortical tonic. The FA group had a longer duration of fever than the other groups and was more likely to have tachycardia. The IANE group was more likely to have a seizure, acute disturbance of consciousness (ADOC), Babinski's sign, and death/sequela (**Table 1**).

Routine Clinical Biochemical Testing

The levels of routine blood, CSF, electrolyte, immune indexes, and blood coagulation were similar among the 4 groups. The ALT, AST, and LDH levels in the IANE group were significantly higher than in the FS and IAE group (**Table 2**).

Specific Biochemical Tests

Serum Test

Except for PDGF-AA, the other 8 serum indicators showed different median variation among each group, but the differences were not statistically significant (**Figure 1**).

CSF Test

The CSF AQP-4 Ab and MDA levels were notably higher in IANE patients in the acute stage compared with FS and IAE (**Figure 2**). At the same time, concentrations of AQP-4 Ab and MDA in plasma were higher than in the CSF ($p<0.001$). Nevertheless, there were not enough samples to test the differences between survivors without sequela and the death/sequela patients in the IANE group.

Neuroimaging and Neuroelectrophysiology

Neuroimaging

Except for the FA group, there were 18 patients with neuroimaging, including 17 brain MRI and 1 brain CT, and 7 patients had positive discoveries. No imaging abnormalities were detected in the FS group. Among the IAE group, 9 patients had imaging examinations, and 2 of them had abnormalities. Brain MRI showed a mild lesion with a reversible splenic lesion (MERS) without follow-up in 1 case (**Figure 3**). Another patient with brain CT over 5 days showed an increased density of the left

Table 1. Demographic and clinical characteristics.

Characteristics, n (%) or as shown	FA, n=4	FS, n=8	IAE, n=14	IANE, n=5
Gender, Male	3 (75)	3 (37.5)	10 (71.4)	2 (40)
Age, years, mean (SD)	5.2 (3.6)	4.1 (2.4)	5.4 (3.3)	3.6 (1.9)
Weight, kg, median (IQR)	15.35 (11.75, 21.85)	15.5 (12, 18.35)	18.5 (13.5, 26)	15 (13, 17)
Onset date				
January	4 (100)	5 (62.5)	7 (50)	3 (60)
December	0 (0)	1 (12.5)	4 (28.57)	1 (20)
Others*	0 (0)	2 (25)	3 (21.43)	1 (20)
Fever, day, median (IQR)	4.5 (4, 9.5)	2 (1, 2)	1 (1, 3)*	3 (1, 4)
Temperature, °C, median (IQR)	39 (39, 39.5)	39.5 (39, 40)	39 (39, 39.25)	39 (39, 39)
Seizure				
No	4 (100)	0 (0)*	3 (21.4)#	0 (0)*,**
1-2	0 (0)	8 (100)	4 (28.6)	1 (20)
≥3	0 (0)	0 (0)	7 (50)	4 (80)
Cough, yes	4 (100)	7 (87.5)	9 (64.3)	3 (60)
Vomiting, yes	1 (25)	0 (0)	6 (42.9)	2 (40)
Sleepiness, yes	2 (50)	2 (25)	4 (28.6)	1 (20)
Somnolence, yes	1 (25)	1 (12.5)	1 (7.1)	1 (20)
ADOC, yes	0 (0)	0 (0)	0 (0)	3 (60)
Alalia, yes	0 (0)	0 (0)	3 (21.4)	1 (20)
Gibberish, yes	0 (0)	0 (0)	3 (21.4)	0 (0)
Babinski's sign, yes	0 (0)	0 (0)	0 (0)	3 (60)
Tachycardia, yes	3 (75)	0 (0)	1 (7.1)	1 (20)
Etiology				
Influenza A	4 (100)	8 (100)	11 (73.3)	4 (80)
Influenza B	0 (0)	0 (0)	4 (26.7)	1 (20)
Treatment				
Oseltamivir/peramivir	4 (100)	7 (87.5)	12 (85.7)	5 (100)
IVIG	2 (50)	0 (0)	5 (35.7)	5 (100)
Glucocorticoids	2 (50)	0 (0)	3 (21.4)	4 (80)
Antibiotics	1 (25)	2 (25)	2 (14.3)	3 (60)
Tracheal intubation ventilator ventilation	0 (0)	0 (0)	0 (0)	2 (40)
Outcome				
Non-survivor/sequela	0 (0)	0 (0)	0 (0)	4 (80)**,**

* FA group were selected as controls and *p*-value <0.0083; ** FS group were selected as controls and *p*-value<0.0083; *** IAE group were selected as controls and *p*-value <0.0083.

Table 2. Biochemical test.

Characteristics, mean (SD) or median (SQR)	FA, n=4	FS, n=8	IAE, n=14	IANE, n=5
Routine blood				
WCB (10 ⁹ /L)	6.5 (2.3)	9.8 (4.3)	7.7 (3.9)	7.5 (3.4)
N (10 ⁹ /L)	4.7 (2.2)	7.5 (4)	5.2 (3)	4.6 (2.9)
L (10 ⁹ /L)	1.1 (0.7, 2)	1.7 (1, 2)	1.2 (0.7, 2.1)	1.8 (1.6, 2.1)
M (10 ⁹ /L)	0.5 (0.4, 0.6)	0.8 (0.4, 1)	0.7 (0.5, 0.9)	0.6 (0.3, 0.9)
Hb (g/L)	119.5 (113, 120.5)	118 (115, 121.5)	124.5 (114, 125)	110 (100, 115)
Plt (10 ⁹ /L)	302.5 (187.5, 402)	235 (213.5, 269.5)	223.5 (200, 280)	232 (225, 271)
CSF				
WBC (10 ⁶ /L)	–	4 (3, 5)	2 (1, 2.5)	1 (1, 2)
HsCRP (mg/L)	–	0.3 (0, 0.3)	0.2 (0, 0.3)	0.2 (0.1, 0.3)
CL (mmol/L)	–	118.2 (118, 126.9)	122.4 (120, 123.2)	123.8 (122, 125.4)
GLU (mmol/L)	–	3.5 (3.2, 3.5)	3.8 (3.4, 4.2)	3.8 (3.4, 4.1)
MP (g/L)	–	0.3 (0.1, 0.3)	0.2 (0.2, 0.3)	0.6 (0.2, 0.7)
LDH (U/L)	–	17 (14, 18)	15 (15, 17)	20 (15, 32)
Electrolyte				
Na (mmol/L)	134.2 (6.4)	132.5 (4.3)	132.1 (4.1)	132.9 (3.2)
K (mmol/L)	3.2 (0.7)	4 (0.7)	3.6 (0.5)	4 (0.4)
BG (mmol/L)	9.2 (6.6, 10.8)	5.6 (5.4, 5.9)	5.1 (4.8, 5.9)	6.4 (6.3, 8.3)
Lac (mmol/L)	1.3 (1.2, 1.5)	1.7 (1.3, 2.1)	1 (0.8, 1.5)	1.5 (1.4, 2.9)
Organ biochemical				
ALT (U/L)	21 (18.5, 42)	14 (12.5, 22)	16.5 (13, 22)	89 (59, 122)*****
AST (U/L)	74 (41.5, 143.5)	36 (31, 43.5)	40 (30, 46)	147 (94, 205)*****
ALT/AST	0.4 (0.3, 0.5)	0.4 (0.4, 0.5)	0.4 (0.3, 0.6)	0.3 (0.3, 1)
LDH (U/L)	415 (383, 508)	248 (239.5, 257)*	269 (214, 290)*	490 (366, 606)*****
CK (U/L)	1632 (253.5, 5235)	165 (147.5, 235.5)	144 (110, 269)	305 (131, 1340)
CK_MB (U/L)	51 (19, 96)	23 (17, 30)	25 (15, 36)	50 (40, 58)
Ammonia (umol/L)	58.8 (45.6)	23.2 (12.4)	29 (8.8)	24.3 (3.7)
Immune indexes				
IgG (g/L)	11.3 (5.3)	10.4 (1.5)	9.7 (2.3)	12.3 (5.7)
IgA (g/L)	1.8 (1)	0.9 (0.3)	1.1 (0.6)	1 (0.8)
IgM (g/L)	1.1 (0.3)	1.6 (0.9)	1.2 (0.3)	1.4 (0.5)
C3 (g/L)	0.9 (0.1)	0.8 (0.1)	0.9 (0.2)	0.8 (0.2)
C4 (g/L)	0.2 (0.1)	0.3 (0.1)	0.2 (0.1)	0.3 (0.1)
IgE (IU/ML)	77 (42.5, 94.5)	60 (31.5, 120)	72.5 (26, 185)	10 (7, 15)

Table 2 continued. Biochemical test.

Characteristics, mean (SD) or median (SQR)	FA, n=4	FS, n=8	IAE, n=14	IANE, n=5
Blood coagulation				
PT (s)	12.9 (12.5, 13.2)	15.1 (14.5, 15.6)	14.5 (13.5, 15)	15.4 (15.2, 16)
APTT(s)	41 (15.3)	46.5 (6)	43.4 (5.6)	44 (9.7)
INR	1 (0)	1.2 (0.1)	1.1 (0.1)	1.2 (0.2)
FIB (g/L)	3.8 (3.4, 4)	2.6 (2.5, 3.3)	2.7 (2.4, 3)	2.5 (2.1, 2.6)

* FA group were selected as controls and p-value <0.0083; ** FS group were selected as controls and p-value<0.0083; *** IAE group were selected as controls and p-value <0.0083.

base section and the two-sided central front-back, then was reviewed using brain MRI that showed no abnormality after 1 week. Imaging examinations were performed in all 5 patients in the IANE group; positive discoveries included 5 cases of bilateral symmetrical lesions, 3 cases of thalamic swelling changes of different degrees, and 2 cases of classical “concentric structure” patterns, and all had multifocal lesions (Figure 4). The non-survivor, who had a Dandy-Walker congenital malformation, developed convulsive persistence and coma after getting influenza; eventually, brain stem failure and death occurred.

Neuroelectrophysiology

There were 8 patients with EEG, and 6 of them had a positive discovery. Abnormal EEG findings in the IAE group included oligorhythmia and frontal intermittent slow waves. In the IANE group, the abnormal EEG showed hypoactivity and partial seizure from the left posterior origin, diffuse delta waves in wakefulness, generalized slow waves, and electrical silence.

Discussion

High-Risk Factors of IANE in Clinical Characteristics

In this study, neurological symptoms/signs appeared in 27 cases and persisted in the IAE and IANE groups. Within 3 days after onset, patients in the IANE group were more likely to have developed multiple seizures, ADOC, and Babinski’s sign, and these problems mostly occurred in young children, whose mean age was 3.6 years in our study. The clinical features above were similar to those in previous reports [12-15]. Therefore, age under 4 years, short-term repeated seizures, ADOC, and Babinski’s sign might be high-risk factors for IANE [6,16,17]. As in previous reports [4,5,13,18-21], the present study did not find any indicators of diagnosis of IANE in routine biochemical examinations, and only showed that the serum levels of ALT, AST, and LDH in the IANE group was significantly higher than in

the FS and IAE groups, and none of these could help diagnose IANE. There was no significant difference in patients who received oseltamivir/peramivir treatment among the 4 groups, suggesting that oseltamivir/peramivir is not effective in preventing IAE and IANE. According to the Consensus Guide, all patients in the IANE group received immunoglobulins (IVIG) and glucocorticoids, but there still was a high mortality rate of 20% and a sequela rate of 60%, which suggests that the diagnosis and treatment of IANE need further attention.

Neuroimaging Findings, Brain Pathology, and Treatment Efficacy in Pathogenesis of IANE

Positive findings in brain imaging are essential indicators for the diagnosis of IANE, which is also known as clinicoradiologic disorder [22]. Like some other reports, our IANE patients also showed the classical neuroimaging, which was “concentric/laminar structure” or “trilaminar pattern” or target-like appearance [23-25]. During the study, other clear “concentric/laminar structure” ANE MRI images were acquired, from whom specimens were not successfully obtained for the biobank, shown in Figure 5. Symmetric necrosis of the thalamus, brain stem, cerebellar medulla, and periventricular white matter had been found in patients with IANE.

The imaging changes in this classic “concentric/laminar structure” can be explained from the brain pathology of the patients with IANE deceased in the acute stage [12,26-28]: moderately sized plasma extravasation occurring around the edge of the lesion, to which the arteries were generally more susceptible than veins, and lesion areas showing myelin pallor; the surrounding tissues of central vessels (arteries, veins, and capillaries) were congested; oligodendrocytes displayed acute swelling; cerebrovascular occlusion, microthrombus formation, and perivascular hemorrhage indicated the central blood vessels were damaged [1,29]; and erythrocyte extravasation was accompanied with neuron and glial cells necrosis, without inflammatory cell infiltration or reactive proliferation of glial cells.

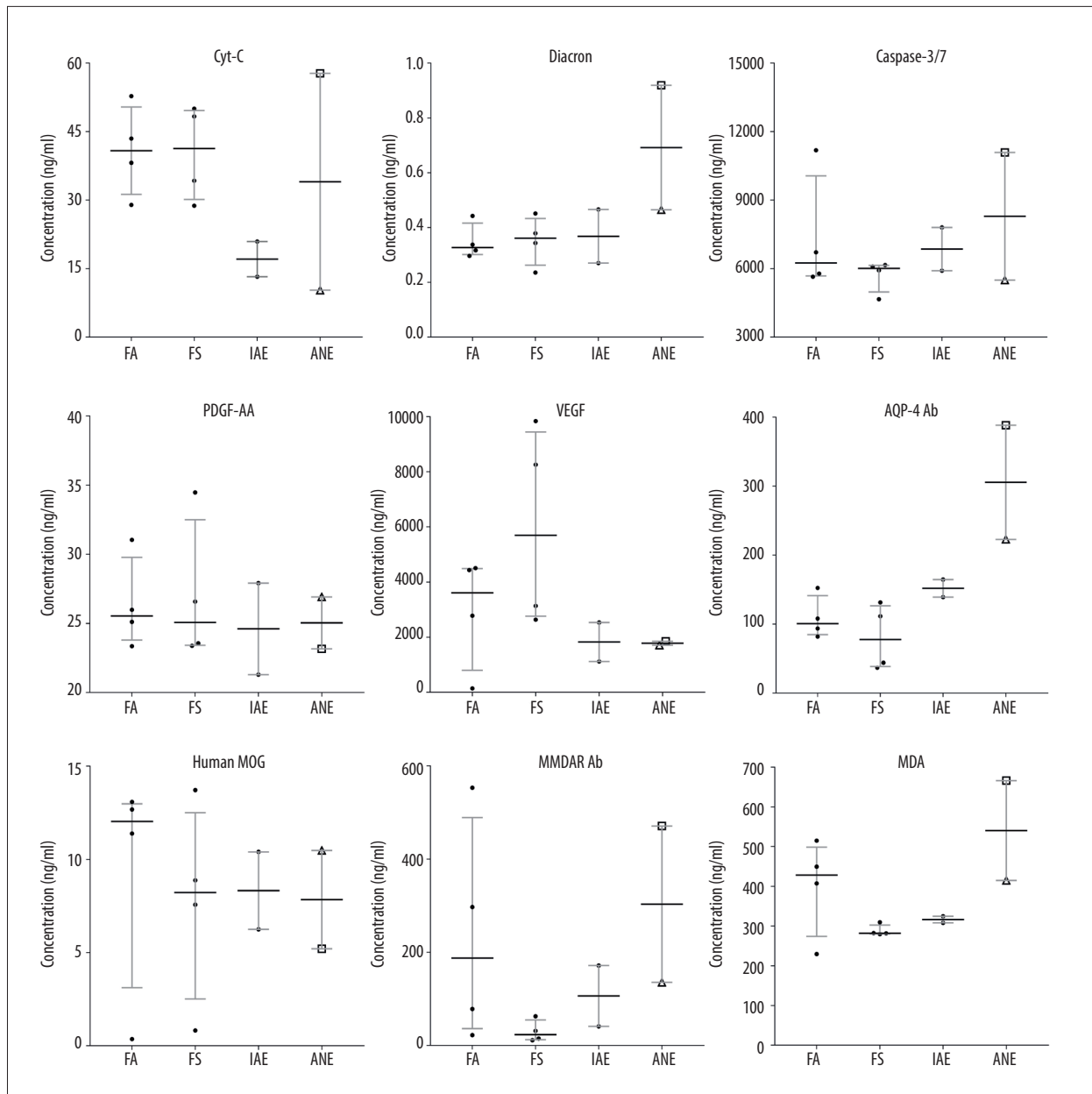


Figure 1. Box and whiskers of specific biochemical serum levels (median+IQR and show all points).

Cerebral hemorrhage and infarction lesions were consistent with autopsy studies of IANE [26,30,31], which matched the area of deep cerebral venous thrombosis (DCVT) shown in **Figure 6**. IANE may share the neuroimaging features of DCVT because thrombosis in the internal cerebral veins, the basal veins, and the great cerebral vein eventually leads to venous (hemorrhagic) infarction and bilateral thalamic vasogenic edema [32]. DCVT can be shown in the magnetic resonance venography (MRV) [33,34].

Still, it is important to make a differential diagnosis between ANE and DCVT. The treatment for ANE, including intravenous

steroids and immunoglobulins, can cause hypercoagulability, and osmotic agents recommended for decreasing intracranial pressure may exacerbate DCVT [20]. Therefore, the high mortality and neurological sequelae after using immunoglobulins and steroids might be related to the absence of early identification of cerebral vascular microembolization/infarction and without subsequent treatment. Bilateral thalamic lesions on the MRI sequence provide an important clue to the diagnosis of DCVT [17,35] and were observed in IANE. Therefore, is DCVT one of the reasons why ANE usually involves bilateral thalamic? Do they share the same or similar mechanism? It is difficult to clearly distinguish ANE from DCVT on clinical

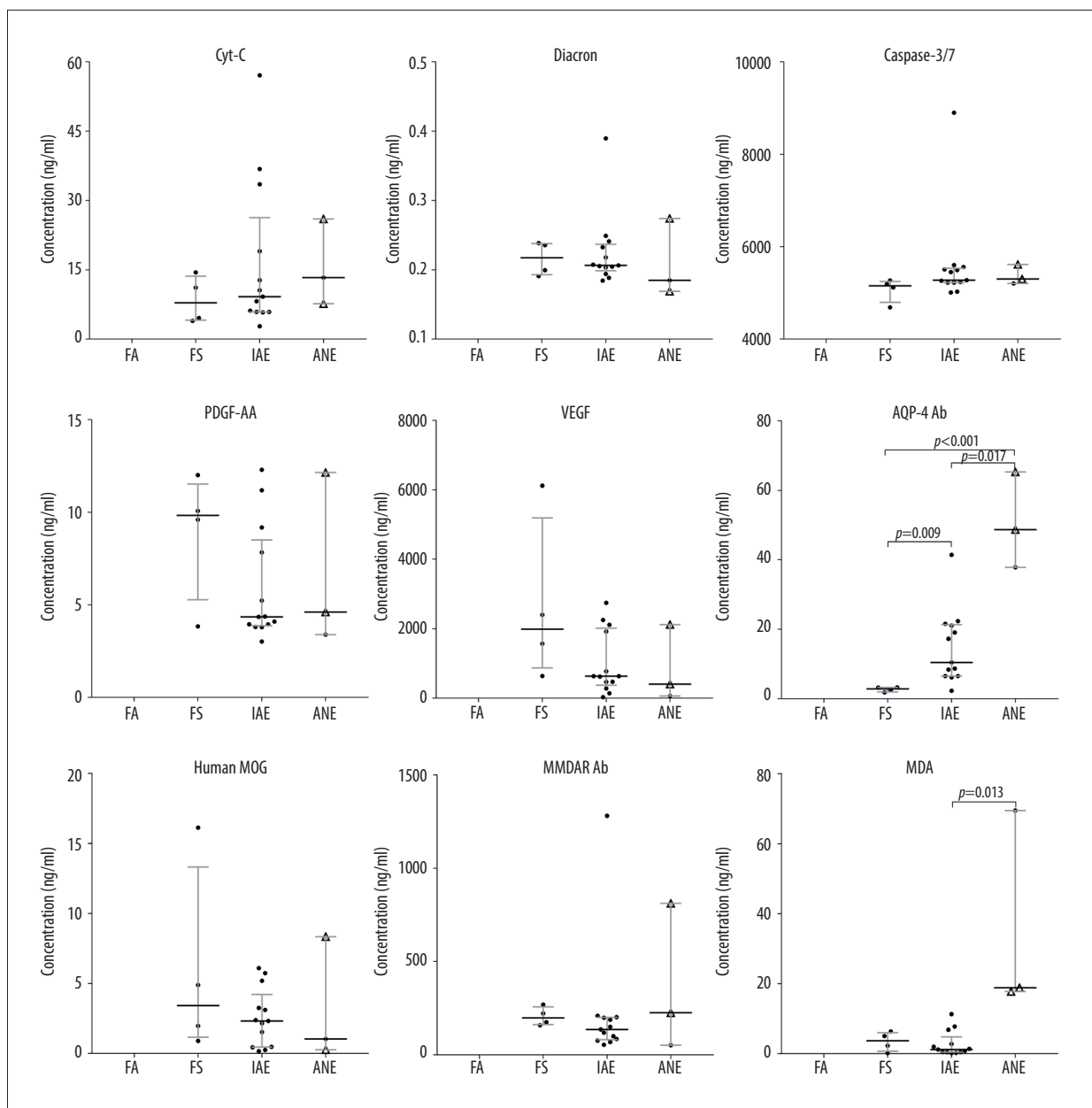


Figure 2. Box and whiskers of specific biochemical CSF levels (median+IQR and show all points).

examination, particularly during influenza infection, because both present with nonspecific symptoms such as alteration of consciousness. Still, magnetic resonance venography (MRV) and susceptibility-weighted imaging (SWI) or T2 sequence can indicate the presence of DCVT [33]. There were no differences in coagulation function among the groups in our study. Thrombelastography (TEG) can be tried to examine the combined effects of various coagulation mechanisms on thrombosis, including the role of blood cells such as platelets, clotting factors, and fibrinolysis [36-39].

Although brain MRI is a diagnostic method for ANE, it could not meet early clinical diagnosis needs. Patients with IANE could miss the opportunity to receive neuroimaging in the acute phase, subject to examination conditions and patient conditions. Because of the imaging lag of brain lesions, neuroimaging cannot provide a clinical judgment of early brain lesions consistent with the actual condition.

Relationship Between Special Biomarkers and IANE

The diagnosis of IANE cannot rely on conventional biochemical indicators, and neuroimaging cannot meet early diagnosis

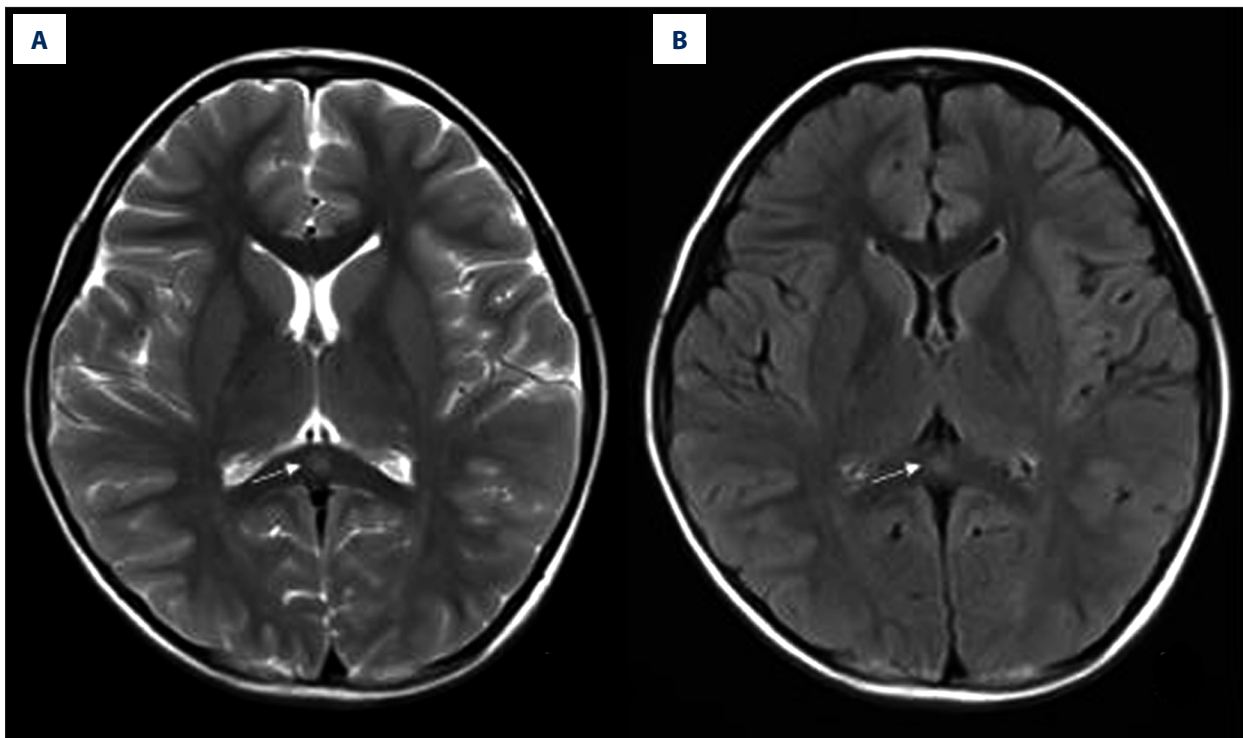


Figure 3. Mild Encephalopathy with a Reversible Splenial (MERS) lesion: Fever 1 day, with 2 seizures. Axial T2WI (A) and T2WI-FLAIR (B) of MRI shows that the small piece of bright signal (arrow) in splenium of corpus callosum; no abnormality was found in the rest of the parenchyma.

needs. To this end, we explored the significance of certain biomarkers for the diagnosis of the disease. Nerve cell necrosis is a major pathological change in IANE, and necrosis-associated biomarkers, including lactate dehydrogenase (LDH) [40-44] and malondialdehyde (MDA) [45-47], are reflected in the CSF. The cytotoxicity is first evaluated by LDH release [48], while MDA is the final cell cracking process [45]. Still, elevated serum LDH due to abnormal liver function common with influenza may interfere with the evaluation effectiveness of CSF-LDH levels on nerve cell necrosis. In this study, the ratio of LDH CSF levels to serum level in patients with IANE sequelae was higher than in the FS and IAE groups. This suggests the usefulness of the biomarker, but it requires confirmation in larger studies. The 4 non-survivor/sequela patients had higher MDA on admission, but there were not enough samples to test the differences between survivors without sequela and the non-survivor/sequela patients.

Still, we found an interesting phenomenon: in the early stage, the ratio of LDH CSF to serum levels in patients with IANE sequelae was higher than the FS and IAE groups (mean=0.091, mean=0.066, mean=0.061, respectively), although there was no significant difference, which might be due to the small sample size. High expression of LDH can occur in cell necrosis [40-44], and the ratio of LDH-CSF/serum could avoid the effect of high LDH serum level caused by liver function damage on its CSF

concentration, which might be used to assess whether the brain cell has necrosis.

The mechanism of nerve cell necrosis in patients with IANE is still unknown. IANE involves a cytokine storm [49,50], but inflammatory cell infiltration and reactive proliferation of glial cells are not found at pathological examination [12,26-28], and Dacron-active oxygen metabolite (d-ROM) and cytochrome c (Cyt-C) had no statistically significant differences in the IANE group in this study, suggesting cytokine factors might not be the main mechanism of IANE. Apoptosis of vascular endothelial cell has been found [51,52], but the level of Caspase-3/7 both in serum and CSF were not confirmed in this study. Studies have shown that both platelet-derived growth factor (PDGF) and vascular endothelial growth factor (VEGF) are elevated in IAE, and elevation of PDGF was correlated with the incidence and prognosis of IANE [53]. However, these were not confirmed in our study. Individuals suffering from autoimmune diseases were more likely to have influenza-associated brain lesions [5,54]. Still, we did not find significant differences between MOG antibody and anti-NMDAR antibody in serum or in CSF.

In this study, the AQP-4 antibody levels in the CSF and plasma were notably increased in IANE patients compared with FS and IAE in the acute stage. AQP-4 is a member of the aquaporin family and has a selective and efficient transmembrane

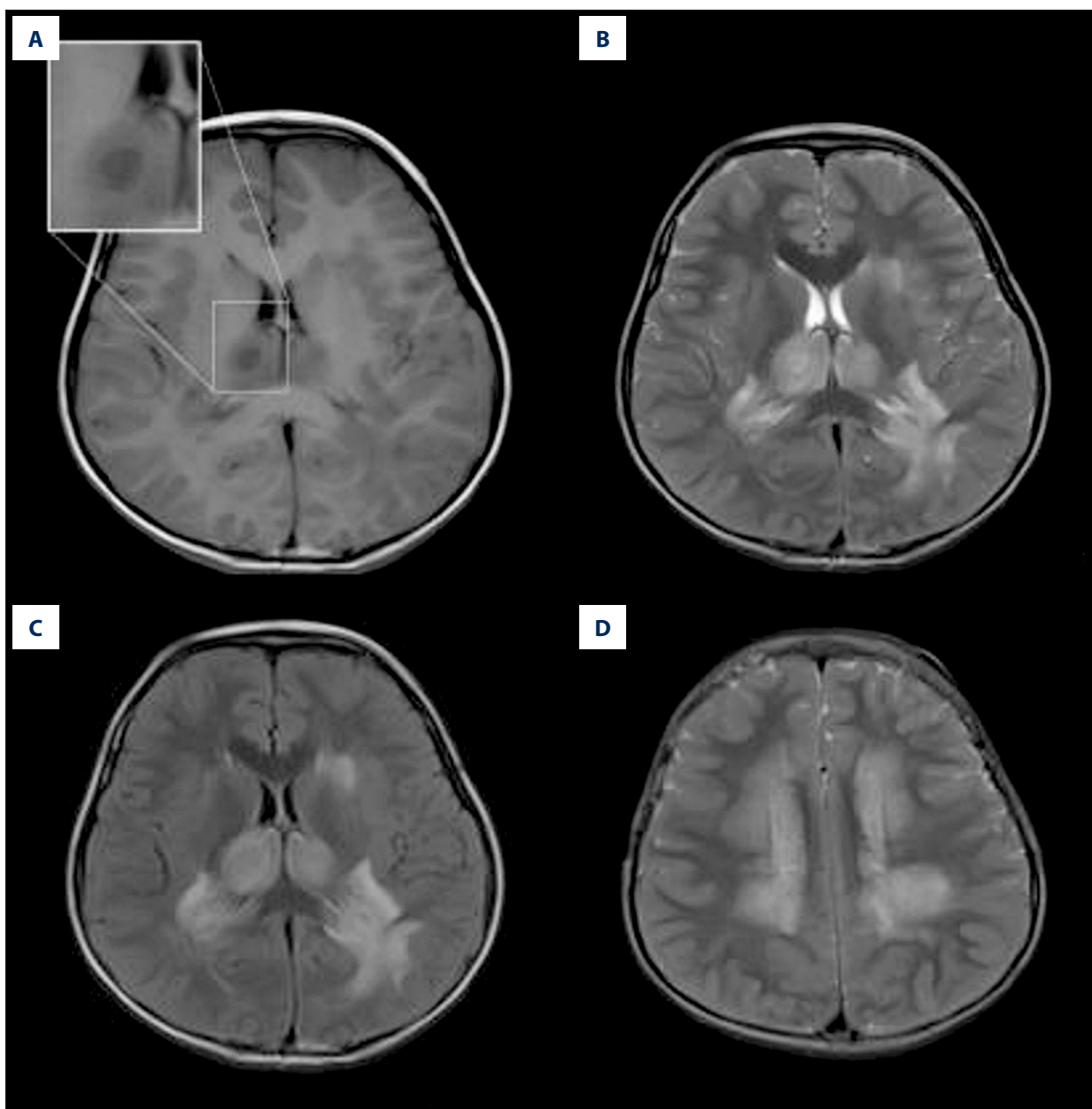


Figure 4. Acute Necrotizing Encephalitis of Childhood (ANE). Fever 1 day, convulsion 3 times. Symmetrical and multifocal involvement were showed in bilateral thalamus and paraventricular (**A**. T1WI, **B**. T2WI, **C**. T2WI-FLAIR) and radial coronal hemispheric center (**D**) white matter with bilateral thalamus swollen.

transport of water molecules [55], is predominantly distributed on the perivascular end-feet of astrocytes [31], and is tightly connected to the microvessels (**Figure 7**) [55,56]. The center of the trilaminar concentric circular structure seen in IANE brain pathology and MRI can be considered as a neurovascular unit (NVU), which consists mainly of microvessels, astrocytes, neurons, extracellular matrix, and other types of gliocytes, and is defined as a completely functional and structural unit of the brain [56]. The fragmented processes of astrocytes in IAE are closely adjacent to synapses on the dendritic spines

with fragmentation [31]. The anti-AQP-4 antibody can mediate neurological diseases such as severe brain edema [57-60]. The brain cell edema rapidly appeared around the pathological microvessels in IANE patients, which might be explained by AQP-4 dysfunction on the astrocyte membrane, but this requires further investigation.

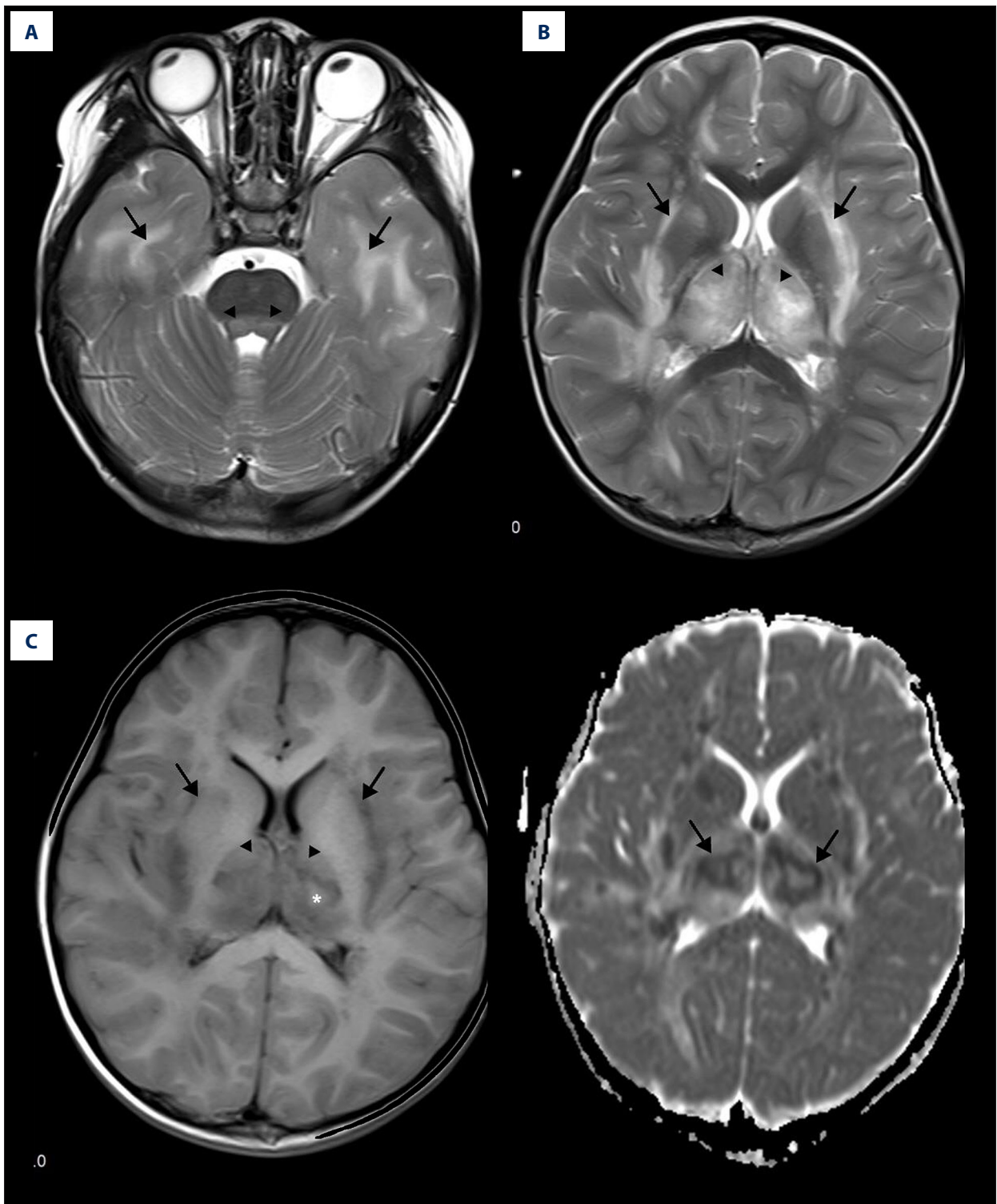


Figure 5. Emesias, febris for 5 days, followed by coma, with throat wrap for influenza type B positive (A–C). (A) Axial T2WI MRI showed mildly higher focal signal intensity in the dorsal aspect of pons (arrow), and mildly higher patchy signal intensity in white matter at bilateral temporal lobe (arrow). (B) Axial T2WI MRI indicated symmetric swelling and higher signal intensity in bilateral thalami (arrow), and white matter in external capsule was involved. (C) Axial T1WI MRI indicated mildly lower signal intensity in bilateral thalami (arrow) with slightly higher signal intensity in center (*), involvement of white matter in external capsule (*) was visible; axial ADC map showed more detailed 3-layer structure of bilateral thalami in ANE (arrow).

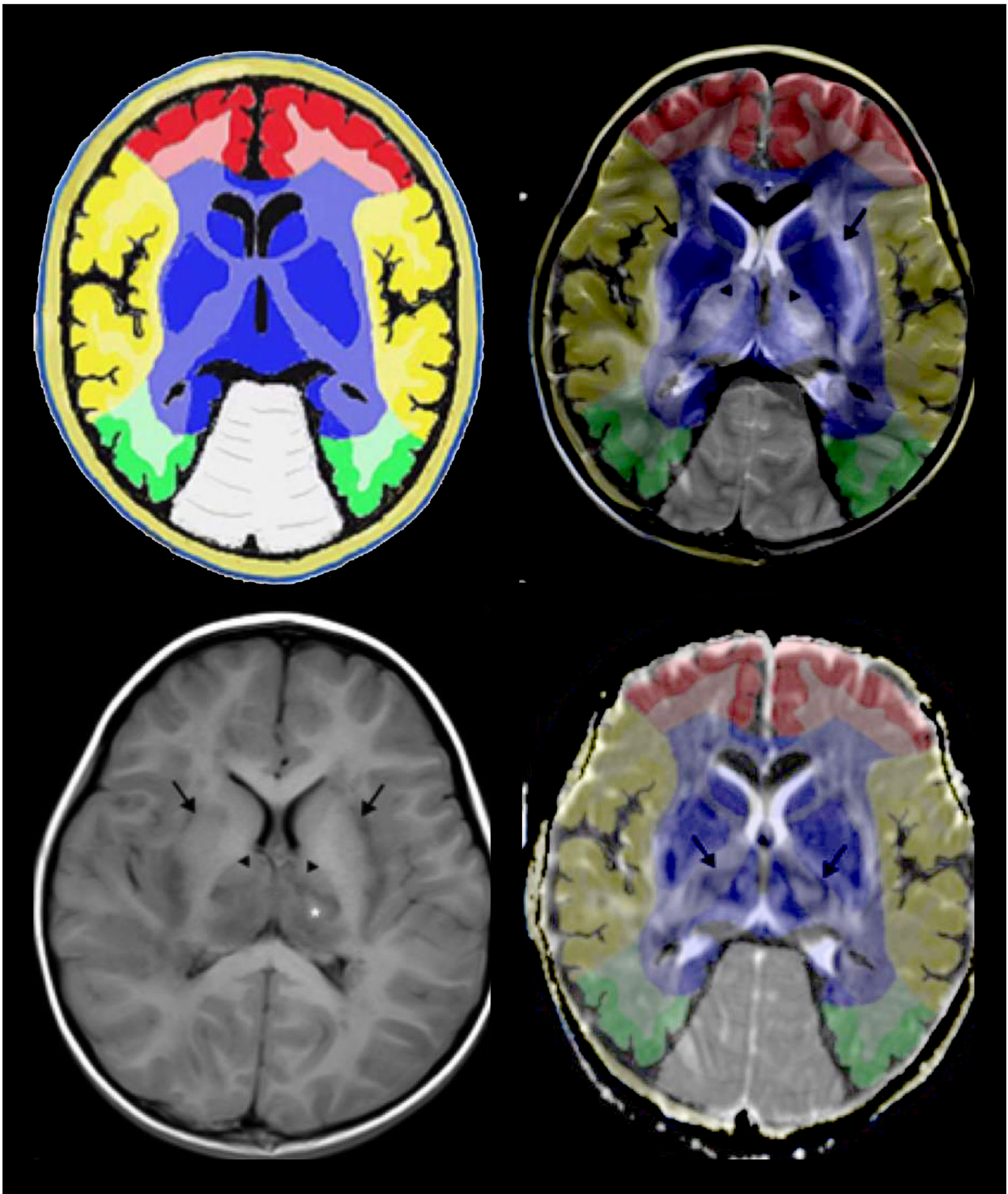


Figure 6. Comparison of brain vascular innervation area and MRI of IANE.

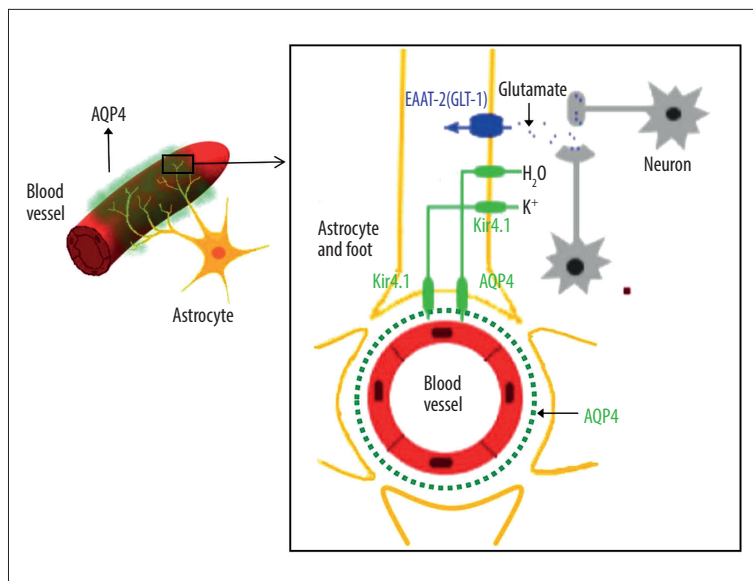


Figure 7. Diagram of the structural relationship between blood vessels, astrocytes, and AQP-4.

Conclusions

Clinical early warning factors for IANE include influenza patients under 4 years of age, rapid occur seizures, ADOC, and pathological signs. CSF levels of AQP-4 antibodies, MDA, and the ratio of LDH-CSF/serum could contribute to the identification of IANE. Neuroimaging shows that IAE and IANE might be diseases with 2 different pathogeneses, and the latter might have the involvement of intracranial vascular factors.

In patients with rapid progression of encephalopathic symptoms, an early nuclear magnetic examination of MRV and SWI sequences, or TEG, can be performed to identify ANE imaging changes caused by DCVT and to guide the clinical strategy.

Conflict of Interest

None.

References:

- Shiomi M. [Pathogenesis of acute encephalitis and acute encephalopathy]. *Nihon Rinsho*. 2011;69:399-408 [in Japanese]
- Okumura A, Abe S, Kidokoro H, et al. Acute necrotizing encephalopathy: A comparison between influenza and non-influenza cases. *Microbiol Immunol*. 2009;53:277-80.
- Howard A, Uyeki TM, Fergie J. Influenza-associated acute necrotizing encephalopathy in siblings. *J Pediatric Infect Dis Soc*. 2018;7:e172-77
- Kondrich J, Rosenthal M. Influenza in children. *Curr Opin Pediatr*. 2017;29:297-302
- Shah S, Keil A, Gara K, et al. Neurologic complications of influenza. *J Child Neurol*. 2014;29:NP49-53
- Wong KK, Jain S, Blanton L, et al. Influenza-associated pediatric deaths in the United States, 2004-2012. *Pediatrics*. 2013;132:796-804
- Chen LW, Teng CK, Tsai YS, et al. Influenza-associated neurological complications during 2014-2017 in Taiwan. *Brain Dev*. 2018;40:799-806
- Togashi T, Matsuzono Y, Narita M, et al. Influenza-associated acute encephalopathy in Japanese children in 1994-2002. *Virus Res*. 2004;103:75-78
- Neilson D. Susceptibility to infection-induced acute encephalopathy 3. In *GeneReviews*(R). Edited by Adam MP, Ardinger HH, Pagon RA, et al. Seattle (WA); 1993
- Mizuguchi M, Hayashi M, Nakano I, et al. Concentric structure of thalamic lesions in acute necrotizing encephalopathy. *Neuroradiology*. 2002;44:489-93
- Wang HS. Concentric thalamic change on MR of acute necrotizing encephalopathy of childhood. *Neuroradiology*. 2003;45:661-62; author reply 663
- Suga K, Mori K. Fatal acute necrotizing encephalopathy: Clinical presentation and imaging findings. *Pediatr Neurol*. 2015;53:93-94
- Mizuguchi M, Abe J, Mikkaichi K, et al. Acute necrotizing encephalopathy of childhood: A new syndrome presenting with multifocal, symmetric brain lesions. *J Neurol Neurosurg Psychiatry*. 1995;58:555-61
- Shirai T, Fujii H, Ono M, et al. A novel autoantibody against ephrin type B receptor 2 in acute necrotizing encephalopathy. *J Neuroinflammation*. 2013;10:128
- Mariotti P, Iorio R, Frisullo G, et al. Acute necrotizing encephalopathy during novel influenza A (H1N1) virus infection. *Ann Neurol*. 2010;68:111-14
- Azziz Baumgartner E, Dao CN, Nasreen S, et al. Seasonality, timing, and climate drivers of influenza activity worldwide. *J Infect Dis*. 2012;206:838-46
- Centers for Disease C, Prevention. Estimates of deaths associated with seasonal influenza – United States, 1976-2007. *Morb Mortal Wkly Rep*. 2010;59:1057-62
- Mungaomklang A, Chomcheoy J, Wacharapluesadee S, et al. Influenza virus-associated fatal acute necrotizing encephalopathy: Role of nonpermissive viral infection? *Clin Med Insights Case Rep*. 2016;9:99-102
- Takanashi J, Barkovich AJ, Yamaguchi K, et al. Influenza-associated encephalitis/encephalopathy with a reversible lesion in the splenium of the corpus callosum: A case report and literature review. *Am J Neuroradiol*. 2004;25:798-802
- Bousser MG, Ferro JM. Cerebral venous thrombosis: an update. *Lancet Neurol*. 2007;6:162-70
- Yamamoto H, Okumura A, Natsume J, et al. A severity score for acute necrotizing encephalopathy. *Brain Dev*. 2015;37:322-27
- Wu X, Wu W, Pan W, et al. Acute necrotizing encephalopathy: An underrecognized clinoradiologic disorder. *Mediators Inflamm*. 2015;2015:792578
- Ormitti F, Ventura E, Summa A, et al. Acute necrotizing encephalopathy in a child during the 2009 influenza A(H1N1) pandemic: MR imaging in diagnosis and follow-up. *Am J Neuroradiol*. 2010;31:396-400

24. Lee YJ, Hwang SK, Kwon S. Acute necrotizing encephalopathy in children: A long way to go. *J Korean Med Sci.* 2019;34:e143
25. Albayram S, Bilgi Z, Selcuk H, et al. Diffusion-weighted MR imaging findings of acute necrotizing encephalopathy. *Am J Neuroradiol.* 2002;25:792-97
26. Chow FC, Edlow BL, Frosch MP, et al. Outcome in patients with H1N1 influenza and cerebrovascular injury treated with extracorporeal membrane oxygenation. *Neurocrit Care.* 2011;15:156-60
27. Ng WF, Chiu SC, Lam DS, et al. A 7-year-old boy dying of acute encephalopathy. *Brain Pathol.* 2010;20:261-64
28. Juan C, Cheng-rong L, Fei-qiu W, et al. [Pathological observation of acute necrotizing encephalopathy associated with 2009 influenza A (H1N1) virus in children.] *Chinese Journal of Practical Pediatrics.* 2012;27:595-98 [in Chinese]
29. Sato T, Moriuchi H. [Influenza-associated encephalopathy]. *Nihon Rinsho.* 2010;68:1661-65 [in Japanese]
30. Dadak M, Pul R, Lanfermann H, et al. Varying patterns of CNS imaging in influenza A encephalopathy in childhood. *Clin Neuroradiol.* 2020;30(2):243-49
31. Tachibana M, Mohri I, Hirata I, et al. Clasmotodendrosis is associated with dendritic spines and does not represent autophagic astrocyte death in influenza-associated encephalopathy. *Brain Dev.* 2019;41:85-95
32. van den Bergh WM, van der Schaaf I, van Gijn J. The spectrum of presentations of venous infarction caused by deep cerebral vein thrombosis. *Neurology.* 2005;65:192-96
33. Taniguchi D, Nakajima S, Hayashida A, et al. Deep cerebral venous thrombosis mimicking influenza-associated acute necrotizing encephalopathy: A case report. *J Med Case Rep.* 2017;11:281
34. Neilson DE. The interplay of infection and genetics in acute necrotizing encephalopathy. *Curr Opin Pediatr.* 2010;22:751-57
35. Sugaya N. Influenza-associated encephalopathy in Japan. *Semin Pediatr Infect Dis.* 2002;13:79-84
36. Curry NS, Davenport R, Pavord S, et al. The use of viscoelastic haemostatic assays in the management of major bleeding: A British Society for Haematology Guideline. *Br J Haematol.* 2018;182:789-806
37. Maegle M, Inaba K, Rizoli S, et al. [Early viscoelasticity-based coagulation therapy for severely injured bleeding patients: Report of the consensus group on the consensus conference 2014 for formulation of S2k guidelines]. *Anaesthesist.* 2015;64:778-94 [in German]
38. Leal-Noval SR, Munoz M, Asuero M, et al. [2013: The Seville document on consensus on the alternatives to allogenic blood transfusion. Update to the Seville document. Spanish Societies of Anaesthesiology (SEDAR), Haematology and Haemotherapy (SEHH), Hospital Pharmacy (SEFH), Critical Care Medicine (SEMICYUC), Thrombosis and Haemostasis (SETH) and Blood Transfusion (SETS)]. *Farm Hosp.* 2013;37:209-35 [in Spanish]
39. Kozek-Langenecker SA, Afshari A, Albaladejo P, et al. Management of severe perioperative bleeding: Guidelines from the European Society of Anaesthesiology. *Eur J Anaesthesiol.* 2013;30:270-382
40. Davitt K, Babcock BD, Fenelus M, et al. The anti-cancer peptide, PNC-27, induces tumor cell necrosis of a poorly differentiated non-solid tissue human leukemia cell line that depends on expression of HDM-2 in the plasma membrane of these cells. *Ann Clin Lab Sci.* 2014;44:241-48
41. Huang CF, Liu SH, Lin-Shiau SY. Pyrrolidine dithiocarbamate augments Hg(2+)-mediated induction of macrophage cell death via oxidative stress-induced apoptosis and necrosis signaling pathways. *Toxicol Lett.* 2012;214:33-45
42. Tran TT, Groben P, Pisetsky DS. The release of DNA into the plasma of mice following hepatic cell death by apoptosis and necrosis. *Biomarkers.* 2008;13:184-200
43. Nakamura H, Mizuno T, Kawamura K, et al. [CSF enzyme activities in patients with head injury – especially on GOT, GPT, LDH, and CPK (AUTHOR'S TRANSL)]. *No Shinkei Geka.* 1976;4: 753-62 [in Japanese]
44. Franke RP, Fuhrmann R, Mrowietz C, et al. Reduced diagnostic value of lactate dehydrogenase (LDH) in the presence of radiographic contrast media. *Clin Hemorheol Microcirc.* 2010;45:123-30
45. Matthews N, Neale ML, Jackson SK, et al. Tumour cell killing by tumour necrosis factor: Inhibition by anaerobic conditions, free-radical scavengers and inhibitors of arachidonate metabolism. *Immunology.* 1987;62:153-55
46. Szymanska JA, Bruchajzer E, Sporny S. Comparison of hepatotoxicity of 1,2-, 1,3- and 1,4-dibromobenzenes: The dynamics of changes of selected parameters of liver necrosis in acute poisoning in mice. *J Appl Toxicol.* 1996;16:35-41
47. Li D, Zhao L, Liu M, et al. Kinetics of tumor necrosis factor alpha in plasma and the cardioprotective effect of a monoclonal antibody to tumor necrosis factor alpha in acute myocardial infarction. *Am Heart J.* 1999;137:1145-52
48. Rakba N, Melhaoui A, Rissel M, et al. Irniine, a pyrrolidine alkaloid, isolated from *Arisarum vulgare* can induce apoptosis and/or necrosis in rat hepatocyte cultures. *Toxicol.* 2000;38:1389-402
49. Kansagra SM, Gallentine WB. Cytokine storm of acute necrotizing encephalopathy. *Pediatr Neurol.* 2011;45:400-2
50. Akiyoshi K, Hamada Y, Yamada H, et al. Acute necrotizing encephalopathy associated with hemophagocytic syndrome. *Pediatr Neurol.* 2006;34:315-18
51. Nakai Y, Itoh M, Mizuguchi M, et al. Apoptosis and microglial activation in influenza encephalopathy. *Acta Neuropathol.* 2003;105:233-39
52. Takahashi M, Yamada T, Nakashita Y, et al. Influenza virus-induced encephalopathy: Clinicopathologic study of an autopsied case. *Pediatr Int.* 2000;42:204-14
53. Morichi S, Morishita N, Takeshita M, et al. Vascular endothelial growth factor (VEGF) and platelet-derived growth factor (PDGF) levels in the cerebrospinal fluid of children with influenza-associated encephalopathy. *J Infect Chemother.* 2017;23:80-84
54. Studahl M. Influenza virus and CNS manifestations. *J Clin Virol.* 2003;28:225-32
55. Assentoft M, Larsen BR, MacAulay N. Regulation and function of AQP4 in the central nervous system. *Neurochem Res.* 2015;40:2615-27
56. Muoio V, Persson PB, Sendeski MM. The neurovascular unit – concept review. *Acta Physiol (Oxf).* 2014;210:790-98
57. Hazell AS. Astrocytes are a major target in thiamine deficiency and Wernicke's encephalopathy. *Neurochem Int.* 2009;55:129-35
58. Jo AO, Ryskamp DA, Phuong TT, et al. TRPV4 and AQP4 channels synergistically regulate cell volume and calcium homeostasis in retinal Müller glia. *J Neurosci.* 2015;35:13525-37
59. Karmacharya MB, Kim KH, Kim SY, et al. Low intensity ultrasound inhibits brain oedema formation in rats: Potential action on AQP4 membrane localization. *Neuropathol Appl Neurobiol.* 2015;41:e80-94
60. Hinson SR, Lennon VA, Pittcock SJ. Autoimmune AQP4 channelopathies and neuromyelitis optica spectrum disorders. *Handb Clin Neurol.* 2016;133:377-403